

Recursive Identification of Cornering Stiffness Parameters for an Enhanced Single Track Model

Christian Lundquist and Thomas Schön

Linköping University Post Print

N.B.: When citing this work, cite the original article.

Original Publication:

Christian Lundquist and Thomas Schön, Recursive Identification of Cornering Stiffness Parameters for an Enhanced Single Track Model, 2009, Proceedings of the 15th IFAC Symposium on System Identification: Vol. 15, Part 1.

<http://dx.doi.org/10.3182/20090706-3-FR-2004.00287>

Copyright: IFAC

Postprint available at: Linköping University Electronic Press

<http://urn.kb.se/resolve?urn=urn:nbn:se:liu:diva-45372>

Recursive Identification of Cornering Stiffness Parameters for an Enhanced Single Track Model^{*}

Christian Lundquist^{*} Thomas B. Schön^{*}

^{*} *Division of Automatic Control, Linköping University,
SE-581 83 Linköping, Sweden, e-mail: {lundquist, schon}@isy.liu.se*

Abstract The current development of safety systems within the automotive industry heavily relies on the ability to perceive the environment. This is accomplished by using measurements from several different sensors within a sensor fusion framework. One important part of any system of this kind is an accurate model describing the motion of the vehicle. The most commonly used model for the lateral dynamics is the single track model, which includes the so called cornering stiffness parameters. These parameters describe the tire-road contact and are unknown and even time-varying. Hence, in order to fully make use of the single track model, these parameters have to be identified. The aim of this work is to provide a method for recursive identification of the cornering stiffness parameters to be used on-line while driving.

Keywords: Recursive estimation, Recursive least square, Vehicle dynamics, Gray box model, Tire-road interaction

1. INTRODUCTION

In Lundquist and Schön [2008a] the authors presented a new approach to estimate the road curvature by fusing the information from a camera, a radar, inertial sensors, a steering wheel sensor and wheel speed sensors, making use of an accurate vehicle model. This model is an enhanced single track model, which is also referred to as the bicycle model in the literature. This model contains several parameters, some of which are known and others that are unknown and hence have to be identified. The cornering behavior of the vehicle is strongly connected to the tire characteristics. The parameters of the tires are often assumed to be constant, and this was also the case in Lundquist and Schön [2008a]. In the present contribution we will show a way to identify these parameters in real time when driving.

To be more specific, the cornering stiffness parameter $C_{\alpha i}$ ($i = f, r$ for the front and the rear tires, respectively) describes the cornering behavior of the tire. The cornering stiffness parameters are used to describe the relation between the lateral friction force of the tires F_i and the slip angles α_i ,

$$F_i = C_{\alpha i} \alpha_i, \quad i = f, r. \quad (1)$$

The slip angle is defined as the angle between the central axis of the wheel and the path along which the wheel moves. Hence, the cornering stiffness parameters have to be included in the model describing the motion of the vehicle. Rather than modeling the cornering stiffness as just a scalar, as indicated in (1), we will model it to be able to account for its dependence of the load transfer from the rear axle to the front axle when braking and vice versa when accelerating. This implies that besides the

lateral and yaw dynamics we have to model the vertical motion of the vehicle as well. In this contribution we will derive a rather simple model for the vertical motion, including only the pitch angle and its derivative. The pitch angle is the angle between ground and the longitudinal axis of the vehicle. In modeling the pitching motion we end up with a linear state-space model, containing several unknown parameters, i.e. it is a linear gray-box model. These parameters can be identified using standard techniques [Ljung, 1999, Graebe, 1990]. Finally, we can make use of the dynamic models describing the pitch, the lateral and the yaw motion of the vehicle to form an appropriate recursive least squares problem for identifying the cornering stiffness parameters on-line.

The problem of estimating the cornering stiffness parameters in the single track model is by no means new. However, our approach is, to the best of the authors knowledge, new in the sense that we make use of the vertical motion as well in order to estimate the stiffness parameters. Furthermore, as a spin-off contribution we provide a way for identifying the pitch dynamics of a vehicle. There are several previous approaches for identifying the cornering stiffness parameters based solely on the lateral dynamics, see e.g. [Wesemeier and Isermann, 2006, Siemel, 1997, Sierra et al., 2006, Baffet et al., 2007]. Grip et al. [2008] used a nonlinear observer to estimate the side slip angle. It is the fact that we have access to measurements of the pitching motion, via the vertical position of the front and the rear suspension, that allows us to take the load transfer into account when identifying the cornering stiffness parameters.

2. LONGITUDINAL AND PITCH DYNAMICS

When a vehicle brakes or accelerates a vertical motion is induced in the vehicle body, the vehicle is said to pitch. This motion does not only depend on the vertical vibration characteristics and the longitudinal brake or drive force, but also on the type of suspension. Nevertheless, we

^{*} This work was supported in part by the the SEnsor Fusion for Safety (SEFS) project within the Intelligent Vehicle Safety Systems (IVSS) program and the strategic research center MOVIII, funded by the Swedish Foundation for Strategic Research (SSF).

will only consider a simple model of the vertical motion, describing how the pitch angle changes over time. In Section 2.1 we provide a brief derivation of the pitch dynamics used in this work, for a more detailed account, see, e.g. Mitschke and Wallentowitz [2004]. There are several unknown parameters in the model of the pitch dynamics that have to be estimated from data. This is the topic of Section 2.2.

2.1 Modeling

In Figure 1 we provide a side view of the vehicle, where the variables necessary for the present derivation are defined. First of all, let us write down the spring and damper equations,

$$F_{zf} = -C_{sf}(z - l_f\chi_f) - C_{df}(\dot{z} - l_f\dot{\chi}_f), \quad (2a)$$

$$F_{zr} = -C_{sr}(z + l_r\chi_r) - C_{dr}(\dot{z} + l_r\dot{\chi}_r), \quad (2b)$$

where C_{sf} , C_{sr} , C_{df} and C_{dr} are the front (f) and the rear (r) spring (s) and damper (d) constants, respectively. The vertical position of the complete chassis is denoted by z . We also assume that the pitch angles are small, implying that $l_i \tan \chi \approx l_i\chi$, $i = f, r$.

The vehicle body's kinetic motion equation in the vertical direction is given by

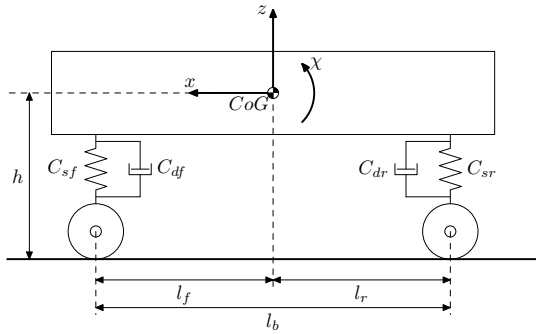
$$m\ddot{z} = F_{zr} + F_{zf}, \quad (3)$$

where F_{zr} and F_{zf} are the vertical spring and damper forces of the front and rear axle, respectively.

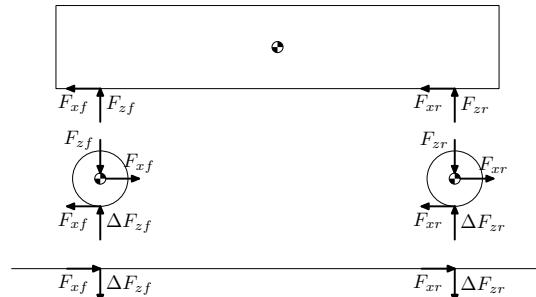
The longitudinal kinetic equation of the vehicle's body is given by

$$m\ddot{x} = F_{xf} + F_{xr} - F_{\text{air}}, \quad (4)$$

where F_{xf} and F_{xr} are the longitudinal forces acting on the wheel traction (positive values) or braking force (negative values) and F_{air} is the drag, given by



(a) Definition of the variables used to describe the vertical motion of the vehicle.



(b) Vertical and longitudinal forces acting on the vehicle, relevant for our model.

$$F_{\text{air}} = c_W A \frac{\rho}{2} v_x^2, \quad (5)$$

where the air density ρ is approximately 1.23 kg/m^3 at 1.0133 bar and 15° [Mitschke and Wallentowitz, 2004]. The cross section is A and the drag coefficient is c_W .

Finally, let us write down the torque equilibrium

$$\ddot{\chi} I_{yy} = -F_{zf} l_f + F_{zr} l_r - (F_{xf} + F_{xr}) h - F_{\text{air}} (h_{\text{air}} - h), \quad (6)$$

where h and h_{air} are the heights of the center of gravity and the center of drag, respectively.

These equations are comprehensive and not all states and parameters are known. Some of the parameters are given by the vehicle manufacturer, other parameters must be identified. Let us first investigate what we know about the vehicle, i.e. what we are measuring with the standard sensors. In our vehicle¹ we measure the following variables related to the longitudinal and the pitch motion,

- the vertical position of the front and the rear suspension, Δz_f and Δz_r ,
- the longitudinal acceleration a_x ,
- the longitudinal velocity v_x and
- the torque and revolution at the internal combustion engine.

The ratio between the front and the rear wheel's longitudinal forces differ depending on whether the vehicle is driving or braking.

The brake force is by construction higher on the front wheels than on the rear wheels. This brake force ratio contributes to a torque around the front wheels. When driving or coasting, the traction forces apply on the driven axle. Our vehicle is all wheel driven and the traction forces on the front and the rear wheels are approximately equal. Hence, the resulting traction force is not applied on the same position as the resulting brake force and in addition whether braking or driving it leads to a non-symmetric pitch behavior.

2.2 Identification

In order to estimate the spring and damper constants, we form a linear gray-box model and the parameters are identified using standard prediction error methods [Ljung, 1999]. In this gray-box model we make use of the suffix χ to clarify that it models the pitch dynamics. Define the states

$$x_\chi = (z \ \dot{z} \ \chi \ \dot{\chi})^T, \quad (7)$$

and the input signals

$$u_\chi = (a_x \ v_x^2)^T. \quad (8)$$

Here it is worth noting that the velocity signal is squared before it is used as an input signal. Finally, the output is defined according to

$$y_\chi = (\Delta z_f \ \Delta z_r)^T. \quad (9)$$

To simplify things, we assume $C_s \triangleq C_{sf} = C_{sr}$ and $C_d \triangleq C_{df} = C_{dr}$. The parameters to be identified are

$$\theta_\chi = (C_s \ C_d \ l_f \ h_{\text{air}})^T. \quad (10)$$

Let us now substitute the traction forces using (4) and the spring and damper forces (2) into (3) and (6) according to

Figure 1. Side view of the vehicle, introducing the variables used to model the vertical motion of the vehicle.

¹ The measurements we collected in cooperation with Nira Dynamics AB using an Audi S3.

$$m\ddot{z} = -(2C_s)z - (2C_d)\dot{z} + (C_s l_f - C_s(l_b - l_f))\varphi + (C_d l_f - C_d(l_b - l_f))\dot{\varphi} \quad (11a)$$

$$I_{yy}\ddot{\chi} = (C_s l_f - C_s(l_b - l_f))z + (C_d l_f - C_d(l_b - l_f))\dot{z} - (C_s l_f^2 + C_s(l_b - l_f)^2)\chi - (C_d l_f^2 + C_d(l_b - l_f)^2)\dot{\chi} - m\ddot{x}h - F_{\text{air}}h_{\text{air}}. \quad (11b)$$

The relation between the pitch angle χ and the measurements y_χ

$$\chi = \arctan\left(\frac{\Delta z_r - \Delta z_f}{l_b}\right) \approx \frac{\Delta z_r - \Delta z_f}{l_b} \quad (12)$$

is used to derive a measurement equation, which together with (11) finally brings us to the state-space model

$$\dot{x}_\chi = \begin{pmatrix} 0 & 1 & 0 & 0 \\ -\frac{2C_s}{m} & -\frac{2C_d}{m} & \frac{C_s l_f - C_s l_r}{m} & \frac{C_d l_f - C_d l_r}{m} \\ C_s l_f - C_s l_r & C_d l_f + C_d l_r & -C_s l_f^2 + C_s l_r^2 & -C_d l_f^2 + C_d l_r^2 \\ I_{yy} & I_{yy} & I_{yy} & I_{yy} \end{pmatrix} x_\chi + \begin{pmatrix} 0 & 0 \\ 0 & 0 \\ 0 & 0 \\ -\frac{mh}{I_{yy}} & -\frac{F_{\text{air}}h_{\text{air}}}{I_{yy}} \end{pmatrix} u_\chi, \quad (13a)$$

$$y_\chi = \begin{pmatrix} 1 & 0 & -l_f & 0 \\ 1 & 0 & l_r & 0 \end{pmatrix} x_\chi, \quad (13b)$$

where $l_r = l_b - l_f$. Measurements with acceleration and brake maneuvers excites the system and are suitable for estimating the parameters. The measurements from the standard sensors are noisy and are therefore filtered before being used for identification purposes. Since the identification can be performed off-line, a zero-phase forward and backward filter is employed. We used two different data sets collected the same day, but on different routes for estimation and validation. More information about the data is presented in Section 5.

A data sequence from the German Autobahn was used to identify the following parameters

$$\begin{aligned} \hat{C}_s &= 8.24 \cdot 10^4, & \hat{l}_f &= 1.45, \\ \hat{C}_d &= 4.45 \cdot 10^3, & \hat{h}_{\text{air}} &= 0.19, \end{aligned}$$

and a validation sequence from a different data set is shown in Figure 2. The raw pitch angle, directly calculated from the measurements using (12) is shown together with the pitch angles computed by our model. Clearly the model match the measurements, indicating that our model is able to capture the pitching dynamics. The corresponding longitudinal acceleration a_x , which is used as input signal to the model is shown in Figure 3. Whenever the vehicle accelerates this will result in a vertical motion, or in other words the pitch angle will change as a result of acceleration. That this is indeed the case for our model should be clear by comparing Figure 2 to Figure 3. For example, at time $t=45$ s there is a negative acceleration (i.e. the vehicle is braking), intuitively this leads to a positive pitching motion (recall the definition of the pitch angle χ in Figure 1(a)).

The input and output signals are corrupted with noise and the state-space model (13) is used within a Kalman filter framework to estimate the states. The load transfer is derived using the spring and damper forces (2) and the estimated states from the Kalman filter according to

$$\Delta F_{zf} = C_{sf}l_f\chi + C_{df}l_f\dot{\chi}, \quad (14a)$$

$$\Delta F_{zr} = -C_{sr}l_r\chi - C_{dr}l_r\dot{\chi}. \quad (14b)$$

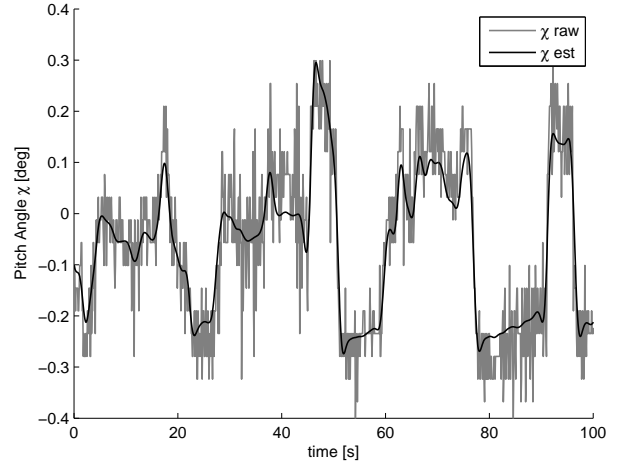


Figure 2. Illustration of the model validation. The gray line corresponds to the raw measurement of the pitch angle, calculated from the measurements using (12). The black line corresponds to the pitch angle produced by the identified model.

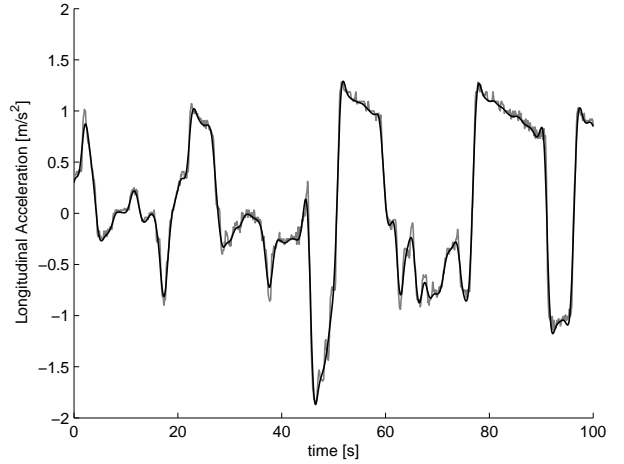


Figure 3. Here the longitudinal acceleration a_x , which is one of the inputs to the model, is shown. The gray line shows the raw measurement signal and the black line shows the filtered signal.

3. LATERAL AND YAW DYNAMICS

We will only be concerned with the vehicle motion during normal driving situations and not at the adhesion limit. This implies that the single track model is sufficient for our purposes [Mitschke and Wallentowitz, 2004]. The geometry of the single track model with slip angles is provided in Figure 4. It is here worth to point out that the velocity vector of the vehicle is typically not in the same direction as the longitudinal axis of the vehicle. Instead the vehicle will move along a path at an angle β with the longitudinal direction of the vehicle. Hence, the angle β is defined as,

$$\tan \beta = \frac{v_y}{v_x}, \quad (15)$$

where v_x and v_y are the vehicle's longitudinal and lateral velocity components, respectively. This angle β is referred to as the float angle [Robert Bosch GmbH, 2004] or the vehicle body side slip angle [Kiencke and Nielsen, 2005]. Lateral slip is an effect of cornering. To turn, a vehicle

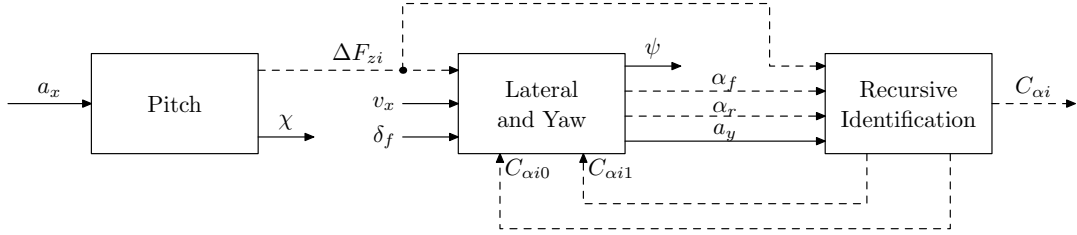


Figure 5. Illustration of our approach to recursive identification of the cornering stiffness parameters. The solid lines corresponds to input signals (arrows pointing to the box) or measurement signals (arrows pointing away from the box) and the dashed lines corresponds to state or parameter estimates that are not directly measured. The pitch dynamics was treated in Section 2 and this is where the load transfer ΔF_{zi} is computed, which is used in forming the regression vector (27). Furthermore, by making use of the lateral and yaw dynamics we can estimate the slip angles and the lateral accelerations which are also needed in solving the recursive identification problem.

$$\tan(\delta_f - \alpha_f) = \frac{\dot{\psi} \cdot l_f}{v_x \cos \beta} + \tan \beta, \quad (30a)$$

$$\tan \alpha_r = -\tan \beta + \frac{\dot{\psi} \cdot l_r}{v_x \cos \beta}. \quad (30b)$$

Under normal driving conditions we can assume small α and β angles, i.e. that $\tan \alpha = \alpha$ and $\tan \beta = \beta$ hold, which results in the following expressions for the slip angles

$$\alpha_f = -\frac{\dot{\psi} \cdot l_f}{v_x} - \beta + \tan \delta_f, \quad (31a)$$

$$\alpha_r = -\beta + \frac{\dot{\psi} \cdot l_r}{v_x}. \quad (31b)$$

This means that we can use the measurements v_x and δ_f and the estimated states $\dot{\psi}$ and β to calculate the slip angles.

4.2 Constrained Recursive Least Squares

The cornering stiffness parameters θ , given in (23), can now be estimated on-line by making use of the recursive solution to the following least squares problem,

$$\hat{\theta} = \arg \min_{\theta \in D_{\mathcal{M}}} \frac{1}{2} \sum_{k=1}^t \lambda^{t-k} (y_k - \varphi_k^T \theta)^T \Lambda^{-1} (y_k - \varphi_k^T \theta), \quad (32)$$

where $0 < \lambda \leq 1$ is the so called forgetting factor. Furthermore, Λ denote a weighting matrix, which can be used to acknowledge the relative importance of the different measurements. It is possible to let λ and/or Λ be time varying. This can for instance be used to model the fact that the parameters are not identifiable during low excitation, i.e., when accelerations or velocities are missing. Finally, $D_{\mathcal{M}}$ is used to denote the set of values over which θ ranges in the given model structure i.e., enforcing constraints on the parameter θ . The unconstrained recursive solution to (32) is given by

$$\hat{\theta}_t = \hat{\theta}_{t-1} + K_t (y_t - \varphi_t^T \hat{\theta}_{t-1}), \quad (33a)$$

$$K_t = P_{t-1} \varphi_t (\lambda_t \Lambda_t + \varphi_t^T P_{t-1} \varphi_t)^{-1}, \quad (33b)$$

$$P_t = \frac{1}{\lambda_t} (P_{t-1} - P_{t-1} \varphi_t (\lambda_t \Lambda_t + \varphi_t^T P_{t-1} \varphi_t)^{-1} \varphi_t^T P_{t-1}). \quad (33c)$$

This is commonly referred to as the recursive least square (RLS) algorithm. For a detailed account of the RLS algorithm and recursive identification in general we refer to Ljung [1999], Ljung and Söderström [1983].

The constraint $\theta \in D_{\mathcal{M}}$ can be enforced by simply projecting the estimates back into $D_{\mathcal{M}}$ when necessary [Ljung, 1999],

$$\hat{\theta}_t = \begin{cases} \hat{\theta}_t & \text{if } \hat{\theta}_t \in D_{\mathcal{M}} \\ \hat{\theta}_{t-1} & \text{if } \hat{\theta}_t \notin D_{\mathcal{M}} \end{cases} \quad (34)$$

5. EXPERIMENTS AND RESULTS

The measurements used to illustrate and evaluate the approach proposed in this work were collected during normal driving conditions. Note that we are only using measurements that are directly available on the CAN bus in our test vehicle.

The cornering stiffness parameters are identified using the RLS algorithm given in (32) using the model given in (22)–(27), with $\Lambda = I$ and $\lambda = 0.99$. Furthermore, the cornering stiffness parameters θ have to belong to the following set $D_{\mathcal{M}}$,

$$\begin{aligned} 20000 < C_{\alpha i} < 120000, \quad i = f, r, \\ \theta > 0, \\ C_{\alpha i0} > C_{\alpha i1}, \quad i = f, r. \end{aligned} \quad (35)$$

The projection (34) is typically active in the beginning of the data sequence or when the system is not excited, i.e. at low velocities or at low lateral accelerations.

Let us start out by providing an illustration of the identified cornering stiffness parameters in Figure 6. The measurements were collected in a test vehicle, which starts from a crossover, accelerates to approximately 100 km/h and follows a rural road for 10 min. Since we do not have access to the true values for the cornering stiffness parameters it is impossible to directly evaluate the accuracy. However, one interesting comparison is made in the figure. That is that there is a significant difference in the value depending on whether the asphalt is dry or wet. This was expected, since the cornering stiffness parameter describes the tire-road contact, which of course varies with wet/dry asphalt. The stiffness is higher on dry asphalt than on a wet and slippery road.

In Figure 7 we try to illustrate the fact that when the longitudinal acceleration is small, the covariance given in (33c) increase and as soon as there is a significant longitudinal acceleration present, the covariance is reduced. This illustrates the excitation problems inherent in this problem.

The slip angles are computed according to (31) and the result is illustrated in Figure 8. Since there are no measurements, we cannot objectively evaluate these estimates.

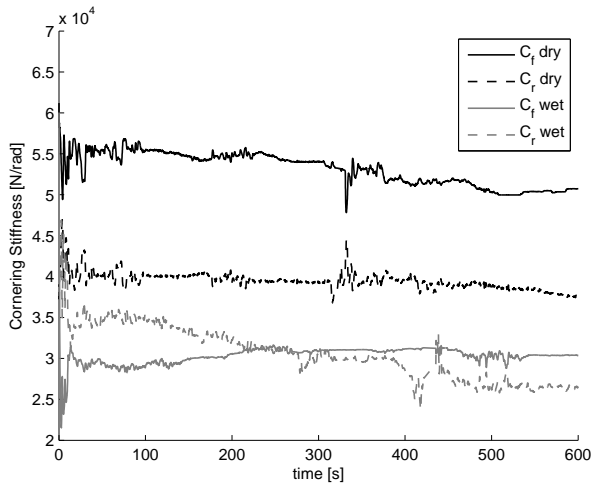


Figure 6. Identified cornering stiffness parameters as a function of time for two different cases, wet and dry asphalt, respectively.

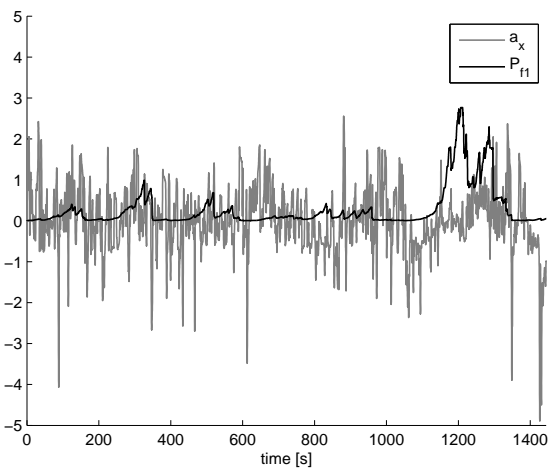


Figure 7. Illustration of the longitudinal acceleration and the covariance associated to the parameter $C_{\alpha f1}$. The plot shows that whenever there is little excitation in the acceleration, the covariance grows and as soon as there is significant acceleration present, the covariance is reduced.

However, based on knowledge about the test drive it can at least be said that the slip angles agrees with the expectation.

The experiments were performed on various public roads in Germany and the results are encouraging. In order to thoroughly validate the results it is necessary to carry out more dedicated experiments and use reference measurement equipment.

6. CONCLUSION

The contribution of this paper is a method for recursive identification of the cornering stiffness parameters that are essential for the single track model. Both the vertical, the lateral and the yaw dynamics are used to form the resulting regression problem that is solved using a constrained RLS algorithm. In order to find the vertical (pitch) dynamics we had to solve a linear gray-box problem. The method has been successfully evaluated on real measurements.

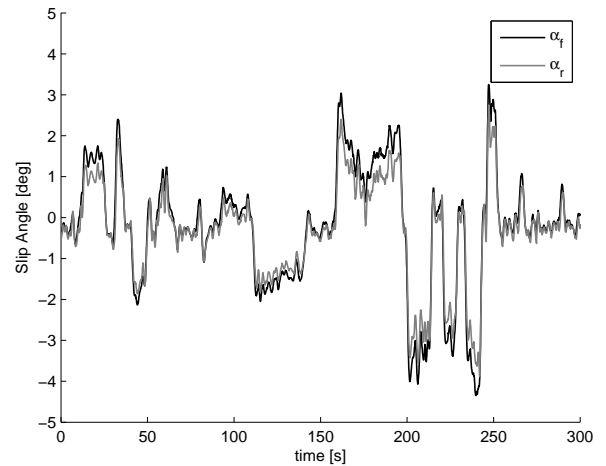


Figure 8. The calculated slip angles during part of the time window used in Figure 7.

ACKNOWLEDGEMENTS

The authors would like to thank Andreas Andersson at Nira Dynamics for fruitful discussions on the German Autobahn and for providing the data.

REFERENCES

- G. Baffet, A. Charara, and D. Lechner. Experimental evaluation of a sliding mode observer for tire-road forces and an extended Kalman filter for the vehicle side slip angle. In *Proceedings of the 46th IEEE Conference on Decision and Control*, pages 3877–3882, New Orleans, LA, USA, December 2007.
- S. Graebe. *Theory and Implementation of Gray Box Identification*. PhD thesis, Royal Institute of Technology, Stockholm, Sweden, June 1990.
- H. F. Grip, L. Imsland, T. A. Johansen, T. I. Fossen, J. C. Kalkkuhl, and A. Suissa. Nonlinear vehicle side-slip estimation with friction adaptation. *Automatica*, 44(3):611 – 622, 2008.
- U. Kiencke and L. Nielsen. *Automotive Control Systems*. Springer, Berlin, Germany, second edition, 2005.
- L. Ljung. *System identification, Theory for the user*. System sciences series. Prentice Hall, Upper Saddle River, NJ, USA, second edition, 1999.
- L. Ljung and T. Söderström. *Theory and Practice of Recursive Identification*. The MIT Press series in Signal Processing, Optimization, and Control. The MIT Press, Cambridge, Massachusetts, 1983.
- C. Lundquist and T. B. Schön. Road geometry estimation and vehicle tracking using a single track model. In *Proceedings of the IEEE Intelligent Vehicles (IV) Symposium*, Eindhoven, The Netherlands, June 2008a.
- C. Lundquist and T. B. Schön. Road geometry estimation and vehicle tracking using a single track model. Technical Report LiTH-ISY-R-2844, Department of Electrical Engineering, Linköping University, Sweden, March 2008b.
- M. Mitschke and H. Wallentowitz. *Dynamik der Kraftfahrzeuge*. Springer, Berlin, Germany, 4th edition, 2004.
- Robert Bosch GmbH, editor. *Automotive Handbook*. SAE Society of Automotive Engineers, 6th edition, 2004.
- W. Sienel. Estimation of the tire cornering stiffness and its application to active car steering. In *Proceedings of the 36th Conference on Decision and Control*, pages 4744–4749, San Diego, CA, USA, December 1997.
- C. Sierra, E. Tseng, A. Jain, and H. Peng. Cornering stiffness estimation based on vehicle lateral dynamics. *Vehicle System Dynamics*, 44(1):24–38, January 2006.
- D. Wesemeier and R. Isermann. Identification of the vehicle cornering stiffness by parallel identification and simulation. In *Proceedings of the 4th IFAC Symposium on Mechatronic Systems*, Heidelberg, Germany, September 2006.